RSC Advances

ROYAL SOCIETY OF CHEMISTRY

www.rsc.org/advances

Origin of arbitrary patterns by direct laser writing in telluride thin film

Tao Wei[1,3], Jingsong Wei[2,*], Kui Zhang[2,3], Qijun Zhou[2,3], Zhen Bai[2,3], Xin Liang[2,3], Qisong Li[1,3], Chenliang Ding[2,3], Yang Wang[2], and Long Zhang[1,**]

[1] Key Laboratory of Materials for High Power Laser, Shanghai Institute of Optics and Fine Mechanics, Chinese Academy of Sciences, Shanghai 201800, PR China

[2]Laboratory for High density optical storage, Shanghai Institute of Optics and Fine Mechanics, Chinese Academy of Sciences, Shanghai 201800, PR China

[3] University of Chinese Academy of Sciences, Beijing 100049, People's Republic of China

[*]weijingsong@siom.ac.cn

[**]lzhang@siom.ac.cn

Abstract

A crystalline telluride (Te) thin film was prepared by radio frequency magnetron controlling sputtering method. Fabrications of arbitrary patterns were achieved successfully by our home-built direct laser writing system in the prepared Te thin film. To elucidate the mechanism of pattern formation, micro X-ray diffraction, micro Raman spectra and micro reflective spectra before and after exposure were analyzed in detail. Results reveal that the occurrence of arbitrary patterns may be ascribed to the decreased grain size in Te thin film, which can further be confirmed by the results of AFM and section images of the Te thin film. It is a simple and cost-effective method for arbitrary pattern fabrications based on the reduction of grain size in laser writing process.

Keywords: Telluride film, crystalline, direct laser writing, arbitrary pattern

1 Introduction

In recent years, much effort has been concentrated on micro-patterns fabrications due to their extensive applications in fields of micro-electronics technology, diffractive optical elements, micro artworks, image storage, *etc*.[1-4]. In this case, Q. Wang et al.

reported optically reconfigurable binary and grayscale devices such as Fresnel zone-plates and super-oscillatory lens[5]. In order to obtain excellent micro-pattern structure, an appropriate fabricating method and photoresist material are both indispensable.

Last decades have witnessed the great development of fabricating techniques, which involve conventional photolithography[6], e-beam or ion-beam lithography[7], nano-imprint[8] and laser direct writing method[9]. However, the low productivity and high cost of e-beam and ion-beam lithography have restrained the practical applications although they have the best fabrication precision. Conventional photolithography and nano-imprint techniques are mostly utilized due to their shorter productive period and large scale manufacturability. Unfortunately, high-cost masks and organic contamination in both methods are not beneficial for their applications. In contrast, laser direct writing technique characterized with the advantages of simple process, maskless fabrication and low cost, has been applied to fabricate micro or nano pattern structures in different materials[10]. Thereby, a home-made direct laser writing setup has been utilized to pattern fabrications.

Besides, a kind of proper photoresist material is required for micro-pattern fabrications. In general, the fabrication of micro/nano patterns needs the following steps involving photoresist, development, and subsequent pattern transfer to underlying substrate. Common photoresist can generate pattern structures based on photochemical changes such as SU-8[11]. Recently, laser thermal lithography technique has also been widely investigated to fabricate micro/nano structures on photoresist, which is mainly based on photo-thermal mode [12-14]. This method has the merits of no optical diffraction limit and low cost. According to laser thermal lithography, photoresist can generate laser thermally induced structure transformation such as phase transition from amorphous to crystalline. Such changes result in different etching rates between exposed and unexposed regions in a given etching solution.

Generally, a suitable photoresist should meet the following conditions: (1) suitable absorption at the specific wavelength, at which the structure of photoresist can change

via light induced thermal effect; (2) clear temperature threshold so as to keep the resist stable below the threshold temperature, while the change of structure such as phase change can occur above the value; (3) good etching resistance beneficial for the pattern transferring from photoresist to underlying substrate. To date, the photoresist materials for micro-pattern fabrications mainly include organic photoresists [11, 15] and chalcogenide materials [16, 17]. Chalcogenide materials are more superior to organic photoresists owing to their broad spectral response, while each organic resist is only sensitive to specific wavelength, which leads to a high investment and a long R&D period[18]. The pre-baking and post-baking steps of organic photoresist can also be omitted so that the procedure of lithography is much simpler for chalcogenide resist[19]. Moreover, chalcogenide resists have smaller fundamental structural units and strong chemical bonds that can make micro-patterns of small and robust structures[20].

So far, chalcogenide materials applied for micro/nano patterns are mainly focused on Sb_2Te_3[21], $Ge_2Sb_2Te_5$[17, 18, 20] and AgInSbTe systems[22]. For example, C.H. Chu, *et al.* reported the fabrication of nano-rings in $Ge_2Sb_2Te_5$ thin film according to the photo-thermal effect of a focused laser beam and subsequent chemical etching[20]. However, its poor surface roughness and blurry patterns after development make $Ge_2Sb_2Te_5$ thin film far from good photoresist. In this case, H. Xi, *et al.* developed successfully a new material $Ge_2Sb_{1.5}Bi_{0.5}Te_5$, which has a smooth surface and a clear edge after the selective etching of KOH solution[18]. Furthermore, high etching selectivity ratio of 524:1 between Si and $Ge_2Sb_{1.5}Bi_{0.5}Te_5$ was also achieved[18]. However, to our knowledge, current chalcogenide system has suffered some bottlenecks such as high-cost and complicated fabrication procedure. Therefore, it is necessary to develop a low-cost and simple material with the good patterning ability.

Actually, chalcogenide materials have been widely researched for applications in flexible optical waveguides, integrated optical circuits[23] and optically reconfigurable metasurfaces and photonic devices[5]. Chalcogenide phase change thin films have also been successfully applied in rewritable optical storage by taking advantage of the optical reflectivity differences between the crystalline and amorphous states induced by

laser pulse radiation[24-26]. Transient super-resolution effect can also be achieved in chalcogenide material[27]. Recently, we have demonstrated the use of chalcogenide materials as greyscale photolithography materials by exploiting four phases of chalcogenide thin films — the liquid and gaseous phases, in addition to the amorphous and crystalline solid phases[21]. Particularly, S. Pleasants reported our work on chalcogenide lithographic and spoke highly of chalcogenide promise for lithography[28]. Additionally, As–S based chalcogenide glass has been used to fabricate microlens array based on photostructural changes, which is similar to organic photoresists[29]. Here, we found another mechanism for chalcogenide lithography, that is, grain refinement leads to smooth surface for pattern lithography.

In this work, Te thin film was selected for pattern fabrications because of its not only simple composition and low cost but also the low melting temperature that is beneficial for energy-saving. Furthermore, the micro-pattern structures of Te thin film can be achieved by only one step without development, pre-baking and post-baking. This paper reported the micro-pattern fabrication of Te thin film via laser direct writing method and the formation mechanism of micro-pattern was also investigated in detail. This work may provide a helpful reference for designing photonic metasurface and devices such as waveguides, grayscale hologram, micro-ring resonators and super-oscillatory lens[30-32].

2 Experimental

2.1 Sample preparations

The Te thin film was deposited on a K9 glass substrate with the thickness of 60 nm which was prepared by radio frequency magnetron controlling sputtering system (JGP560 type) at room temperature. The background pressure was approximately 4×10^{-4} Pa. The sputtering power was 20 W and the working gas was Ar with the pressure of 0.7 Pa.

2.2 Pattern structure fabrications

A home-made setup of diode-based high-speed rotation-type direct laser (405 nm wavelength) writing system (SpinDWL405) with the numerical aperture (NA) of 0.65

was used to write pattern structures directly on Te thin films in air. Pulsed-wave mode was adjusted by a signal generator. Laser power, pulse width and writing speed were tuned in the system. In this study, the laser power was fixed at ~0.5 mW and pulse width was 30 ns, respectively. The writing speed is fixed at 3 m/s.

2.3 Pattern characterizations

The micro X-ray diffraction (XRD) data (exposure and unexposed regions) and absorption spectra from 250 to 800 nm were recorded via 18KW-D/MAX2500V type equipment produced by Rigaku and UV-Vis-NIR spectrophotometer, respectively. The fabricated patterns were observed by optical microscope (Olympus BX51 microscopy) and scanning electronic microscopy (SEM) (Zeiss Auriga with focusing ion beam milling system, Carl Zeiss, Germany), respectively. In order to investigate the mechanism of pattern formation, micro reflection and micro Raman spectra between exposure and unexposed regions were obtained by micro-reflection spectrum (PG2000-Pro, Idea Optics Company, China) and Renishaw Micro-Raman Spectroscopy System with excitation wavelength of 785 nm, respectively. An atomic force microscope (AFM, Multimode V, Veeco) with tip in tap mode was used to observe the morphology of the directly written pattern structures. All measurements were carried out at room temperature.

3 Results and discussion

In our work, the semiconductor laser diode with 405 nm wavelength was used for pattern writing, which was based on the facts that its production cost has decreased significantly in the last few years thanks to technological progress and mass production. According to the direct laser writing system (SpinDWL405), arbitrary patterns have been fabricated successfully in a Te thin film. It is noted that the laser energy density is as low as 7.6×10^{-6} J·mm^{-2}, which is much lower than those of Sn (3×10^{-2} J·mm^{-2}) and $Ge_2Sb_{1.5}Bi_{0.5}Te_5$ thin films (1.31×10^{2} J·mm^{-2}) [18, 33]. This suggests that Te thin films possess the merit of energy-saving.

3.1 Optical microscopy and SEM images

Fig.1 shows the optical images of laser-writing micro-hexagonal stars, micro-snowflakes, micro-gears and SEM pattern of micro-hexagonal stars. For comparison, the original pictures of hexagonal star, snowflake and gear are displayed in the inset of Fig.1 (a), (b) and (c), respectively. It can be seen from Fig. 1 (a), (b) and (c) that pattern structures are clear and very similar to the original pictures, as indicated in the inset of Fig. 1 (a)-(c). The results indicate that Te thin film can be utilized as a photoresist material for micro-pattern fabrication. Scanning electron microscopy (SEM) of studied samples allowed us to see the surface structure and morphology of the films. The SEM image in Fig. 1 (d) displays the clear micro-hexagonal stars from Fig.1 (a), which shows flat surface with no obvious concave or convex shape. In order to achieve the practical applications of Te thin film, it is necessary to shed light on the mechanism of pattern formation. Therefore, optical absorption spectra (250~800 nm) and micro-XRD (exposure and unexposed parts) results were determined, which is indicated in Fig.2.

3.2 Absorption spectra and micro-XRD analysis

In Fig. 2(a), effective absorption of Te film from 300 to 800 nm can be observed, especially for the 405 nm wavelength. However, the glass substrate (K9 glass) has no absorption in the wavelength range. Therefore, Te thin films based on photo-thermal effect can be suitable for optical lithography. Fig. 2(b) shows characteristic diffractive peaks in both unexposed and exposed regions, which both correspond to hexagonal Te nanocrystals (PDF#36-1452). It is noted that peak positions have no evident changes in both regions. These results suggest that the Te thin film has no phase transformation before and after exposure. In addition, the XRD results also indicate the nature of crystal state of as-deposited (unexposed region) Te thin film.

However, diffractive peak intensity after exposure is slightly lower than that in unexposed regions. This phenomenon may be ascribed to the reduction of grain size and low crystallinity. For the purpose of further examining the obtained results, micro-Raman spectra (50-200 cm^{-1}) in exposure and unexposed regions of a hexagonal star pattern are given, as shown in Fig. 3(a) and (b).

3.3 Micro-Raman and micro-reflective spectra

In combination of Fig. 3(a) and (b), it is found that two obvious Raman peaks at 127 cm^{-1} and 145 cm^{-1} occur in as-deposited Te thin film, which correspond to two vibration mode (A_1 and E_{TO} mode) of Te-Te bond, respectively[34]. After exposure, the intensity of two peaks have no significant changes while the peak positions both shift to low wavenumber region, at 121 cm^{-1} and 140 cm^{-1}, respectively. It is reported that Raman shift is closely related to grain size of the material [35, 36]. Smaller grain size leads to Raman shift to lower wavenumber [35, 36]. It is believed in our work that Raman shift from high wavenumber to low wavenumber is due to the decreased grain size of Te thin film.

Fig. 3(c) gives the micro-reflective spectra (400-800 nm) in exposure and unexposed regions of a hexagonal star pattern. It is evident that the reflectivity of exposed regions higher apparently than that of unexposed regions. It is considered that laser exposure makes grains smaller and small grains rearrange closely, which makes the surface of Te thin film smoother after exposure and thus leads to lower light scattering and higher reflectivity.

3.4 AFM image analysis

In order to further confirm the proposed view, AFM image of lantern structure (Fig. 4(b)) and the section image were obtained, which is indicated in Fig. 4(a) and (c). The exposed and unexposed regions are marked as ‘1’ and ‘2’, respectively, as shown in Fig. 4(a). One can see that the surface of region ‘1’ is smoother than that of region ‘2’. The cross-section image of Fig. 4(c) signifies that the average surface roughness of region ‘1’ is 0.5 nm, which is apparently lower than that of region ‘2’ (5.5 nm). According to Ref.[37-39], it is proposed that the reduction of grain size leads to the decrease of surface roughness in Te thin film. Therefore, the reduction of grain size after laser exposure is the origin of pattern formation in Te thin film.

4 Conclusions

In conclusion, arbitrary patterns such as hexagonal stars, snowflakes and gears have been fabricated successfully by a direct laser writing setup in a crystalline Te thin film.

Micro XRD results indicate that the Te crystalline remains the same after exposure. However, the reflectivity of exposed region is higher than that of unexposed region. Micro-Raman spectra indicate Raman shift from high wavenumber to low wavenumber after exposure, which is ascribed to the reduction of grain size in Te thin film. AFM image and section analysis further indicate that the reduction of surface roughness is due to the smaller grain size in the writing process. This work may provide a meaningful reference for future fabrication of functional devices such as Fresnel zone plates, super-oscillatory lens and greyscale holograms based on chalcogenide materials.

Acknowledgements

This work was partially supported by the National Natural Science Foundation of China (Nos. 51172253 and 61137002).

References

1. C. F. Guo, Z. Zhang, S. Cao and Q. Liu, *Opt. Lett.*, 2009, **34**, 2820-2822.
2. S. Juodkazis, V. Mizeikis and H. Misawa, *J. Appl. Phys.*, 2009, **106**, 051101.
3. C. Rizza, E. Palange and A. Ciattoni, *Photonics Res.*, 2014, **2**, 121-125.
4. R. Li, Z. Guo, W. Wang, J. Zhang, K. Zhou, J. Liu, S. Qu, S. Liu and J. Gao, *Photonics Res.*, 2015, **3**, 252-255.
5. Q. Wang, E. T. F. Rogers, B. Gholipour, C.M. Wang, G. Yuan, J. Teng and N. I. Zheludev, *Nat. Photonics*, 2015, **10**, 60-65.
6. S. Hashioka and H. Matsumura, *Jpn. J. Appl. Phys.*, 2000, **39**, 7063.
7. F. Watt, A.A.Bettiol, J. A. V. Kan, E. J. Teo and M. B. H. Breese, *Int. J. Nanosci.*, 2005, **4**, 269–286.
8. K.-S. Han, J.-H. Shin, W.-Y. Yoon and H. Lee, *Sol. Energy Mater. Sol. Cells,* 2011, **95**, 288-291.
9. W. Yu, X. Yuan, N. Ngo, W. Que, W. Cheong and V. Koudriachov, *Opt. Express*, 2002, **10**, 443-448.

10. C. F. Guo, V. Nayyar, Z. Zhang, Y. Chen, J. Miao, R. Huang and Q. Liu, *Adv. Mater.* 2012, **24**, 3010-3014, 3076.

11. A. Rammohan, P. K. Dwivedi, R. Martinez-Duarte, H. Katepalli, M. J. Madou and A. Sharma, *Sens. Actuators, B*, 2011, **153**, 125-134.

12. Y. Usami, T. Watanabe, Y. Kanazawa, K. Taga, H. Kawai and K. Ichikawa, *Appl. Phys. Express*, 2009, **2**, 126502.

13. C. P. Liu, C. C. Hsu, T. R. Jeng and J. P. Chen, *J. Alloys Compd.*, 2009, **488**, 190-194.

14. Y. C. Lee, S. Chao, C. C. Huang and K. C. Cheng, *Opt. Express*, 2013, **21**, 23556-23567.

15. C. Deng, Y. Geng and Y. Wu, *J. Mater. Chem.*, 2013, **1**, 2470.

16. O. Shiman, V. Gerbreders, A. Gerbreders and V. Kolbjonoks, *J. Non-Cryst. Solids,* 2013, **377**, 165-168.

17. J. Li, L. Zheng, H. Xi, D. Liu, H. Zhang, Y. Tian, Y. Xie, X. Zhu and Q. Liu, *Phys. Chem. Chem. Phys.*, 2014, **16**, 22281-22286.

18. H. Xi, Q. Liu, Y. Tian, Y. Wang, S. Guo and M. Chu, *Opt. Mater. Express*, 2012, **2**, 461-468.

19. Y. Kumaresan, A. Rammohan, P. K. Dwivedi and A. Sharma, *ACS Appl. Mater. Interfaces*, 2013, **5**, 7094-7100.

20. C. H. Chu, M. L. Tseng, C. D. Shiue, S. W. Chen, H.P. Chiang, M. Mansuripur and D. P. Tsai, *Opt. Express*, 2011, **19**, 12652-12657.

21. R. Wang, J. Wei and Y. Fan, *Opt. Express*, 2014, **22**, 4973-4984.

22. A. Dun, J. Wei and H. Zhao, *Mater. Lett.*, 2012, **66**, 324-327.

23. C. Ríos, M. Stegmaier, P. Hosseini, D. Wang, T. Scherer, C. D. Wright, H. Bhaskaran and W. H. P. Pernice, *Nat. Photonics*, 2015, **9**, 725-732.

24. T. Matsunaga, J. Akola, S. Kohara, T. Honma, K. Kobayashi, E. Ikenaga, R. O. Jones, N. Yamada, M. Takata and R. Kojima, *Nat. Mater.*, 2011, **10**, 129-134.

25. J. Hegedus and S. R. Elliott, *Nat. Mater.*, 2008, **7**, 399-405.

26. A. V. Kolobov, P. Fons, A. I. Frenkel, A. L. Ankudinov, J. Tominaga and T. Uruga, *Nat. Mater.*, 2004, **3**, 703-708.

27. X. Zhang and J. Wei, *Photonics Res.*, 2015, **3**, 100-105.

28. S. Pleasants, *Nat. Photon*, 2014, **8**, 352-352.

29. A. Kovalskiy, M. Vlcek, H. Jain, A. Fiserova, C. M. Waits and M. Dubey, *J. Non-Cryst. Solids*, 2006, **352**, 589-594.

30. J. Cheng and N. Yan, *Chin. Opt. Lett.*, 2015, **13**, 082201.

31. L. Li, H. Lin, S. Qiao, Y. Zou, S. Danto, K. Richardson, J. D. Musgraves, N. Lu and J. Hu, *Nat. Photonics*, 2014, **8**, 643-649.

32. M. Z. Ali, A. A. Bhatti, Q. u. Haque and S. Mahmood, *Chin. Opt. Lett.*, 2015, **13**, 090601.

33. J. Zhang, C. Guo, H. Zhang and Q. Liu, *Nanoscale*, 2013, **5**, 8351-8354.

34. A. S. Pine and G. Dresselhaus, *Phys. Rev. B*, 1971, **4**, 356-371.

35. J. Zi, H. Büscher, C. Falter, W. Ludwig, K. Zhang and X. Xie, *Appl. Phys. Lett.*, 1996, **69**, 200-202.

36. C. C. Yang and S. Li, *J. Phys. Chem. B*, 2008, **112**, 14193-14197.

37. J. B. Boyce, G. B. Anderson, D. K. Fork, R. I. Johnson, P. Mei and S. E. Ready, *Mater. Res. Soc. Symp. Proc.*, 1994, **321**, 671.

38. A. Marmorstein, A. T. Voutsas and R. Solanki, *J. Appl. Phys.*, 1997, **82**, 4303-4309.

39. X. H. Wu, D. Kapolnek, E. J. Tarsa, B. Heying, S. Keller, B. P. Keller, U. K. Mishra, S. P. DenBaars and J. S. Speck, *Appl. Phys. Lett.*, 1996, **68**, 1371-1373.

Figure captions

Fig.1 Optical images of (a) micro-hexagonal stars, (b) micro-snowflakes, (c) micro-gears and (d) SEM patterns of micro-hexagonal stars in Te thin film by laser direct writing method. The original images of hexagonal star, snowflake and gear are also given in the insets of (a), (b) and (c), respectively.

Fig.2 (a) Absorption spectra, (b) XRD curves in Te thin film via unexposed and exposed conditions.

Fig.3 (a) The enlarged optical image of a micro hexagonal star, (b) micro Raman spectra in exposure and unexposed regions and (c) micro reflective spectra in exposure and unexposed regions.

Fig. 4 (a) AFM pattern of (b) lantern structure and (c) the section image in the Te thin film.

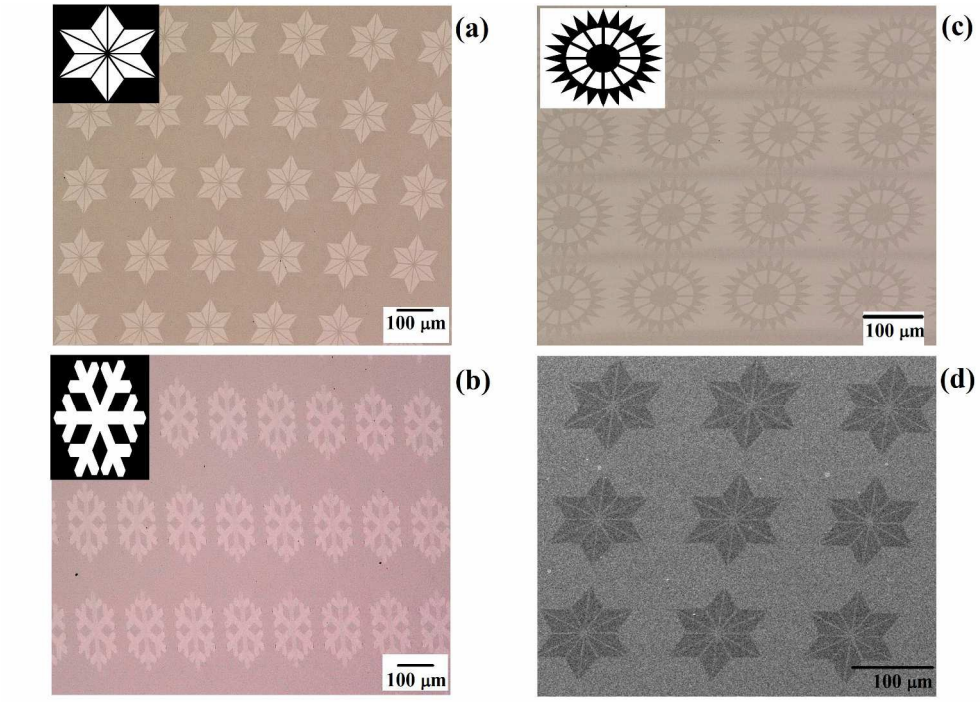

Fig.1 Optical images of (a) micro-hexagonal stars, (b) micro-snowflakes, (c) micro-gears and (d) SEM patterns of micro-hexagonal stars in Te thin film by laser direct writing method. The original images of hexagonal star, snowflake and gear are also given in the insets of (a), (b) and (c), respectively.
287x201mm (300 x 300 DPI)

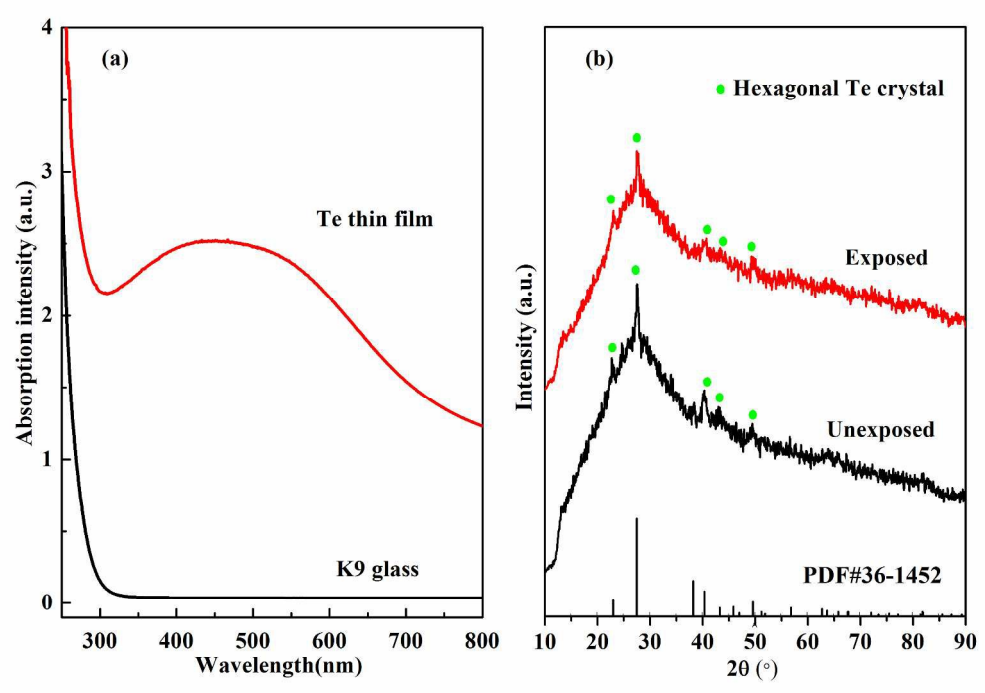

Fig.2 (a) Absorption spectra, (b) XRD curves in Te thin film via unexposed and exposed conditions.
287x201mm (300 x 300 DPI)

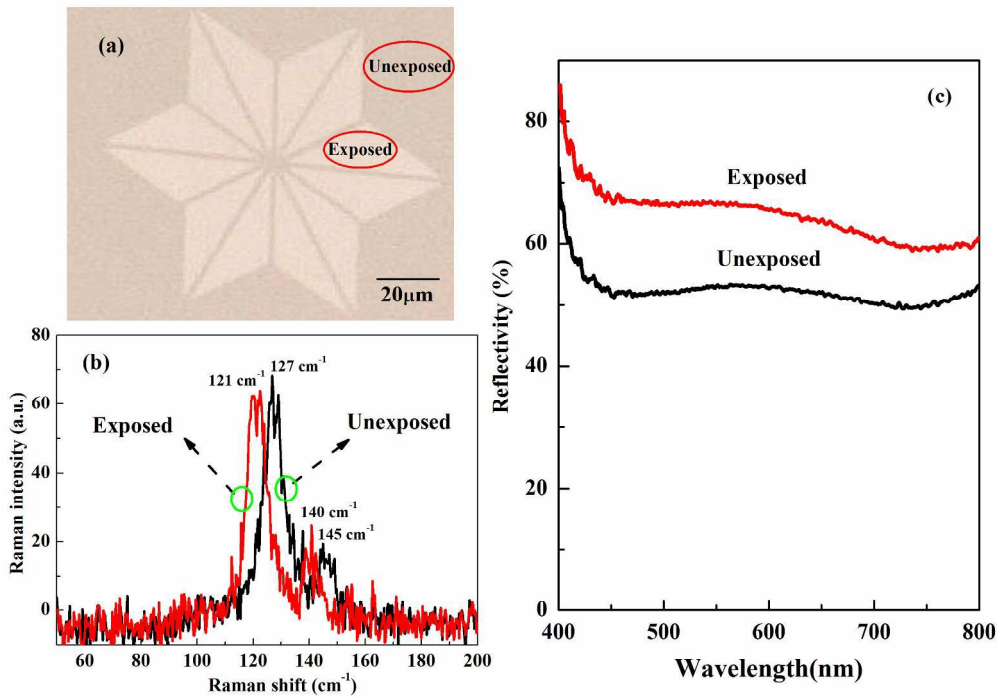

Fig.3 (a) The enlarged optical image of a micro hexagonal star, (b) micro Raman spectra in exposure and unexposed regions and (c) micro reflective spectra in exposure and unexposed regions.
287x201mm (300 x 300 DPI)

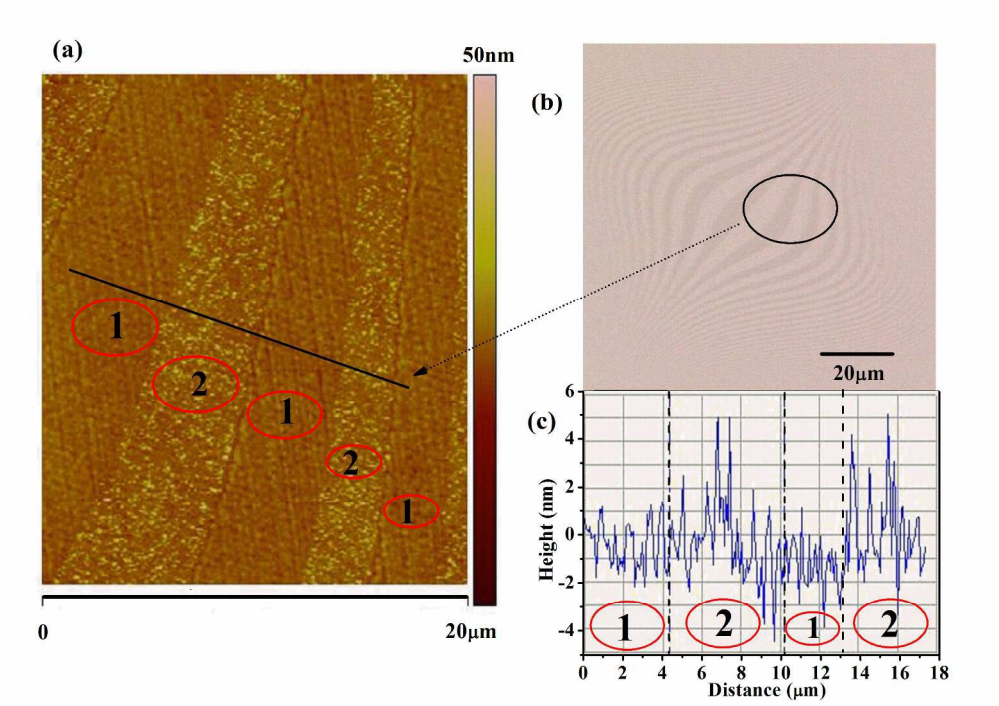

Fig. 4 (a) AFM pattern of (b) lantern structure and (c) the section image in the Te thin film.
296x209mm (300 x 300 DPI)

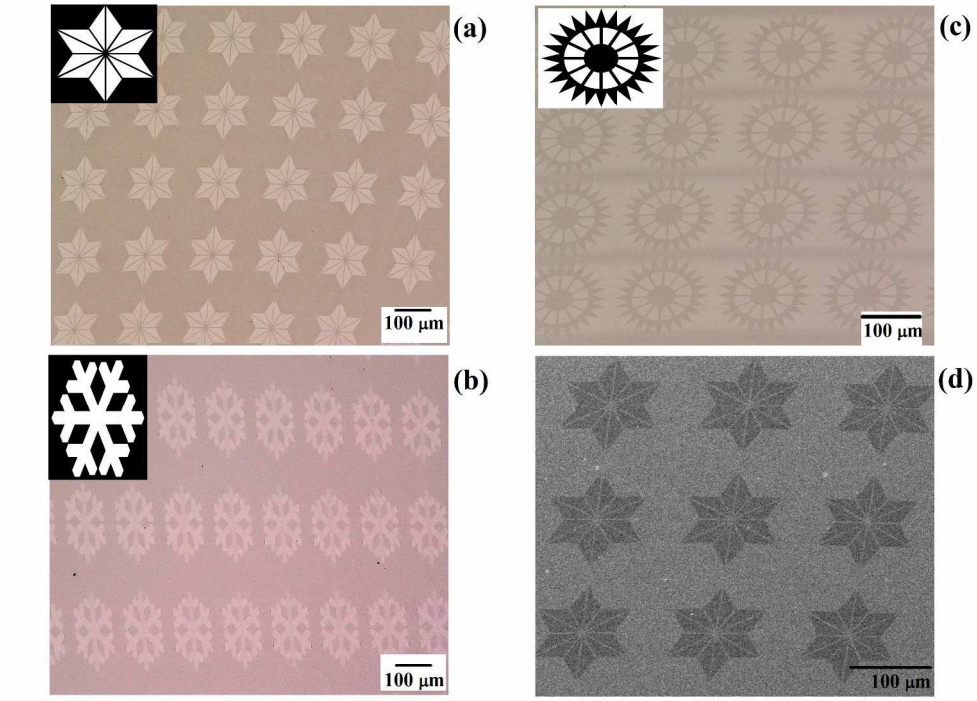

287x201mm (300 x 300 DPI)